On solving the singular system arisen from Poisson equation with Neumann boundary condition

Myoungho Yoon, Gangjoon Yoon and Chohong Min

March 22, 2016

Abstract

We consider solving the singular linear system arisen from the Poisson equation with the Neumann boundary condition. To handle the singularity, there are two usual approaches: one is to fix a Dirichlet boundary condition at one point, and the other seeks a unique solution in the orthogonal complement of the kernel. One may incorrectly presume that the two solutions are the similar to each other. In this work, however, we show that their solutions differ by a function that has a pole at the Dirichlet boundary condition. The pole of the function is comparable to that of the fundamental solution of the Laplace operator. Inevitably one of them should contain the pole, and accordingly has inferior accuracy than the other. According to our novel analysis in this work, it is the fixing method that contains the pole.

The projection method is thus preferred to the fixing method, but it also contains cons: in finding a unique solution by conjugate gradient method, it requires extra steps per each iteration. In this work, we introduce an improved method that contains the accuracy of the projection method without the extra steps. We carry out numerical experiments that validate our analysis and arguments.

1 Introduction

In this article, we consider the Poisson equation with the Neumann boundary condition

$$\begin{cases} -\Delta u = f & \text{in } \Omega \\ \frac{\partial u}{\partial n} = g & \text{on } \partial\Omega. \end{cases} \tag{1}$$

Compared to the Dirichlet problem, the Neumann problem has two distinct features. One is the following so-called compatibility condition

$$\text{(compatibility condition)} \quad \int_\Omega f\,dx + \int_{\partial\Omega} g\,ds = 0 \tag{2}$$

that necessarily holds for the existence of a solution. The other is the non-uniqueness of solution. We need to put an extra condition for its uniqueness such as

$$\begin{array}{rl} \text{(mean zero)} & \int_\Omega u\,dx = 0, \text{ or} \\ \text{(fixing one point)} & u = 0 \text{ at some } Q \in \Omega. \end{array}$$

Though there are numerous numerical methods for solving the Neumann problem such as finite difference methods, finite element methods and finite volume methods, most of them inevitably face solving singular linear system, since the addition of arbitrary constant to the solution makes another solution. Let

$$A^h u^h = b^h \tag{3}$$

be the linear system induced by any of them, then the kernel space $\ker(A^h)$ is generated by a constant function.

To handle the singularity, there are two practical methods [9]. One is to assign a Dirichlet boundary condition at a point $Q \in \Omega^h$:

$$\text{(Fixing one point method)} \qquad \begin{cases} A^h u_F^h = b^h & \text{in } \Omega^h \setminus \{Q\} \\ u_F^h(Q) = 0. \end{cases} \tag{4}$$

The other is based on the fact that b^h may not be in the range space $R(A^h)$. Let P^h be the projection matrix onto the range space $R(A^h)$. For the existence of solution, $P^h b^h$ is taken instead of b^h, and for the uniqueness, solution is chosen from $\ker(A^h)^\perp$, that is, the mean zero solution is chosen, $\sum_{X\in\Omega^h} u_P^h(X) = 0$:

$$\text{(Projection method)} \qquad \begin{cases} A^h u_P^h = P^h b^h & \text{in } \Omega^h \\ u_P^h \in \ker(A^h)^\perp. \end{cases} \tag{5}$$

Each of the two methods succeeds in converting the singular system into a nonsingular one. Each seems to be reasonable and proper on its own way, and one may incorrectly presume that the two solutions are the similar. However, their behaviors are different, as we shall show by the analysis and argument in Section 2 and the numerical experiments in Section 4.

Remark Another method for solving the singular system is to solve an augmented system

$$\begin{bmatrix} A^h & 1^h \\ (1^h)^T & 0 \end{bmatrix} \begin{bmatrix} u^h \\ c \end{bmatrix} = \begin{bmatrix} b^h \\ 0 \end{bmatrix}$$

Here and hereafter 1^h denotes the vector with all components equal to one. The augmented matrix is symmetric and non-singular, but it fails to be positive-definite though A^h is semi-positive. We note that the scalar c is given as the mean of b^h, so that the solution of the augmented system is the same as that of the projection method [20, 6].

2 Numerical analysis

In this section, we compare the numerical performances of the projection and one-point fixing methods. Each method seems to be reasonable and proper on its own way, and two solutions may be misunderstood as the same, but the behaviors of the two solutions are surprisingly different. To explain the phenomena, we focus on the standard finite difference method in the unit volume in $\mathbb{R}^2$. Our analysis in the special cases shows that the two solutions differ by a function that is comparable to the fundamental solution of the Laplace operator, which has a pole at the point where the Dirichlet boundary condition is improved Other numerical methods seem to behave similarly, which will be presented with numerical evidences in Section 4.

To this end, we consider the Poisson equation only in rectangular domains in $\mathbb{R}^2$ and $\mathbb{R}^3$. With a grid node set Ω^h, let $-\Delta^h$ be a discrete Laplacian obtained by the standard finite difference method.

2.1 Analysis in L^2 norm

In this subsection, we compare the behavior of the two methods applied to the standard 5-point finite difference method in the unit rectangle. Even though the analysis is carried out only for unit rectangle in $\mathbb{R}^2$, its estimate turns out to be valid for general domains in $\mathbb{R}^2$ and $\mathbb{R}^3$, which is validated by numerical experiments in Section 4.

In this work, $\langle\cdot,\cdot\rangle_h$ denotes the L^2 inner product defined by $\langle u, v\rangle_h = \sum_{(x_i,y_j)\in\Omega^h} u_{ij}v_{ij}h^2$ and $\|\cdot\|_{L^2}$ is the norm induced by the L^2 inner product.

With $b^h = (b_{ij})$, the one-point fixing method finds a solution $u_F^h \in \mathbb{R}^{N\times N}$ ($N = 1/h$) by choosing a point $Q = (x_{i_0}, y_{j_0}) \in \Omega^h$ arbitrarily and taking $u_F^h(Q) = 0$. That is, u_F^h can be obtained by solving the consistent linear equation as follows.

Lemma 2.1 *Let u_F^h be the discrete solution to Equation* (4)*. Then u_F^h satisfies the equation*

$$A^h u_F^h = b^h - \left\langle 1^h, b^h \right\rangle_h \delta_Q^h \quad \text{in } \Omega^h, \tag{6}$$

where the Dirac delta function δ_Q^h is defined as $\delta_Q^h(X) = 1/h^2$ (and $1/h^3$ for the three dimensional case) if $X = Q$ and $\delta_Q^h(X) = 0$ otherwise.

Proof From Equation (4), it is enough to show that $A^h u_F^h(Q) = b^h(Q) - \left\langle 1^h, b^h \right\rangle_h \frac{1}{h^2}$. The facts that A^h is symmetric and $\ker(A^h) = \mathit{span}\{1^h\}$ imply the range space $R(A^h)$ of A^h is given by $R(A^h) = \left\{1^h\right\}^\perp$. Since $A^h u_F^h \in R(A^h)$, $\left\langle A^h u_F^h, 1^h \right\rangle_h = 0$, and then we have

$$0 = A^h u_F^h(Q)\, h^2 + \sum_{X \in \Omega^h \setminus \{Q\}} A^h u_F^h(X) h^2 = A^h u_F^h(Q)\, h^2 + \sum_{X \in \Omega^h \setminus \{Q\}} b^h(X) h^2.$$

So $A^h u_F^h(Q) = -\sum_{X \in \Omega^h \setminus \{Q\}} b^h(X) = -\left\langle 1^h, b^h \right\rangle_h \frac{1}{h^2} + b^h(Q)$, and we show the lemma. ∎

On the other hand, the projection method is to find a solution u_P^h in the orthogonal complement $\left\{1^h\right\}^\perp$ satisfying

$$A^h u_P^h = P^h b^h \quad \text{in } \Omega^h, \tag{7}$$

where P^h is the projection matrix onto $\left\{1^h\right\}^\perp$ given by $P^h = \mathbf{I} - h^2 1^h \left(1^h\right)^T$, with the identity matrix $\mathbf{I}$ on $\mathbb{R}^{N \times N}$. In this case, we can see that the matrix equation is represented as $P^h A^h P^h u_P^h = P^h b^h$ and $P^h b^h = b^h - \left\langle b^h, 1^h \right\rangle_h 1^h$.

Let G_h be a discrete function such that

$$\left\langle G^h, 1^h \right\rangle_h = 0 \quad \text{and} \quad A^h G^h = \delta_Q^h - 1^h. \tag{8}$$

Then we have

$$u_P^h - u_F^h = \left\langle 1^h, b^h \right\rangle_h G^h - \left\langle 1^h, u_F^h \right\rangle_h 1^h \tag{9}$$

by using $\ker(A^h) = \mathit{span}\{1^h\}$ and taking the inner product with 1^h.

Thus, the estimation of G^h gives that of the difference $u_P^h - u_F^h$ of the two solutions. For the estimation, we need the following lemmas.

Lemma 2.2 *For a given discrete function u^h, we cannot have a maximum of u at a point X where $-\Delta^h u^h(X) < 0$.*

Proof Let $X = (x_i, y_j)$ be a point where u has its maximum. then the Laplacian $-\Delta^h u^h(X)$ is valued as

$$-\Delta^h u^h(X) = \frac{1}{h^2} \left[\begin{array}{ll} \alpha_{i+\frac{1}{2},j}(u_{i,j}^h - u_{i+1,j}^h) & +\alpha_{i-\frac{1}{2},j}(u_{i,j}^h - u_{i-1,j}^h) \\ +\alpha_{i,j+\frac{1}{2}}(u_{i,j}^h - u_{i,j+1}^h) & +\alpha_{i,j-\frac{1}{2}}(u_{i,j}^h - u_{i,j-1}^h) \end{array} \right],$$

where the coefficients $\alpha_{i\pm\frac{1}{2},j}$ and $\alpha_{i,j\pm\frac{1}{2}}$ are nonnegative. So $-\Delta^h u^h(X)$ should be nonnegative. ∎

Applying Lemma 2.2 to G^h in Equation (8) shows $G^h(X) \le G^h(Q)$ for all $X \in \Omega^h$. The following is a discrete-type Sobolev inequality which plays an important role in this work. For the proof, we refer to Lemma 3.4 and its proof in [3] for the two dimensional case and Lemma 5.1 and its proof in [2] for the three dimensional case.

Lemma 2.3 *Let Ω be the unit volume in $\mathbb{R}^d$, $d = 2, 3$. Then, there exists a constant $C > 0$ independent of h such that for any $X \in \Omega^h$ and for all discrete function u^h defined on Ω^h, we have*

$$\|u^h - \bar{u}\|_\infty^2 \le \begin{cases} C\,(1 + |\ln h|)\, \|\nabla^h u^h\|_{L^2}^2, & \text{for } d = 2, \\ C h^{-1} \|\nabla^h u^h\|_{L^2}^2, & \text{for } d = 3, \end{cases} \tag{10}$$

for $\bar{u} = \left\langle u^h, 1^h \right\rangle_h$ or $\bar{u} = u^h(X)$, where ∇^h is the difference operator induced by the standard centered finite difference.

A simple computation by exchanging the order of summation shows that the discrete integration-by-parts holds in this setting [21].

Lemma 2.4 (Discrete Integration by Parts) *For any discrete functions u^h and v^h on Ω^h, we have*

$$\left\langle A^h u^h, v^h \right\rangle_h = \left\langle \nabla^h u^h, \nabla^h v^h \right\rangle_h .$$

Lemma 2.5 *Let b^h be the discrete vector given in Equation* (3)*. Then we have,*

$$\left\langle b^h, 1^h \right\rangle_h = O(h^2).$$

Proof Let u^h be a discrete solution to Equation (3). Since

$$\left\langle b^h, 1^h \right\rangle_h = \left\langle A^h u^h, 1^h \right\rangle_h \approx \int_\Omega f\, dx + \int_{\partial\Omega} g\, ds,$$

the compatibility condition (2) and the $O(h^2)$ accuracy of the midpoint numerical itegration show the lemma. ∎

Using the discrete function G^h, we have the following estimate for the gradient of the difference $(u_F^h - u_P^h)$ for the discrete solutions u_F^h and u_P^h.

Theorem 2.6 *With u_F^h and u_P^h given in Equation* (6) *and* (7)*, respectively, we have*

$$\|\nabla_h (u_F^h - u_P^h)\|_{L^2} = \begin{cases} O\left(h^2\sqrt{1+|\ln h|}\right) & \text{in } [0,1]^2 \\ O\left(h^{1.5}\right) & \text{in } [0,1]^3 . \end{cases}$$

Proof First, we consider the two dimensional case. Let G^h be the discrete function given in Equation (8). Applying Lemmas 2.3 and 2.4 to G_h gives

$$\|G^h\|_\infty^2 \le C(1+|\ln h|)\|\nabla^h G^h\|_{L^2}^2 \le C(1+|\ln h|)\|G^h\|_\infty.$$

That is, we obtain an upper bound for G^h as

$$|G^h(X)| \le C\left(1+|\ln h|\right) \quad \text{for all } X \in \Omega^h.$$

for some constant $C > 0$ independent of h. Recall the relation in Equation (9)

$$u_P^h - u_F^h = \left\langle 1^h, b^h \right\rangle_h G^h - \left\langle 1^h, u_F^h \right\rangle_h 1^h.$$

Using $\|\nabla^h G^h\|_{L^2}^2 = \left\langle G^h, A^h G^h \right\rangle_h = G^h\left(Q\right)$ and Lemma 2.5, we have an estimate for the gradient of $u_F^h - u_P^h$ as

$$\|\nabla^h (u_P^h - u_F^h)\|_{L^2} = \left\langle 1^h, b^h \right\rangle_h \|\nabla_h G_h\|_{L^2} \le C \cdot O(h^2)\sqrt{1+|\ln h|}.$$

For the three dimensional case, replacing the upper bound $(1+|\ln h|)$ by $1/h$ in Lemma 2.3 and applying the same arguments to unit cube in $\mathbb{R}^3$, we obtain the result. ∎

2.2 Argument in L^∞ norm

In this subsection, we compare the two solutions u_P^h and u_F^h, and estimate the size of their difference in L^∞ norm. Though their difference could be sometimes unnoticeable in L^2 norm, the estimation will show that the difference is quite large in L^∞, which will be validated by numerical tests in Section 4.

In the previous subsection, we showed that $u_P^h - u_F^h + \left\langle 1^h, u_F^h \right\rangle_h 1^h = O\left(h^2\right) G^h$. We may assume the fixing point $Q \in \Omega_h$ to be the origin. The discrete function G^h is determined by the equation $A^h G^h = \delta^h - \frac{1^h}{\langle 1^h, 1^h \rangle_h}$, which corresponds to the following discrete boundary problem.

$$\begin{cases} -\Delta^h G^h &= \delta^h - \frac{1^h}{\langle 1^h, 1^h \rangle_h} \quad \text{in } \Omega^h, \\ \frac{\partial G^h}{\partial n} &= 0 \quad \text{on } \partial\Omega^h, \\ \left\langle G^h, 1^h \right\rangle_h &= 0. \end{cases}$$

In the continuous analysis point of view, the discrete boundary problem obviously approximates the following continuous boundary problem, whose solution is the so-called Neumann function G [12].

$$\begin{cases} -\Delta G &= \delta - \frac{1}{\int_\Omega dx} \quad \text{in } \Omega, \\ \frac{\partial G}{\partial n} &= 0 \quad \text{on } \partial\Omega, \\ \int_\Omega G\, dx &= 0. \end{cases}$$

It is known that the Neumann function G has a pole of singularity that is comparable to that of the fundamental solution of the Laplace operator [1]. Being an approximation of the Neumann function, G^h around the point at which Dirichlet boundary condition is posed is expected to behave much like the discrete fundamental solution around the origin. The discrete fundamental solution F^h is defined by the equation

$$-\Delta^h F^h = \delta^h \text{ in } (h\mathbb{Z})^d \quad (\delta^h = \frac{1}{h^d}\delta).$$

The discrete fundamental solution is known to have a singularity at the origin. It grows to the infinity as fast as the function $\log\left(\sqrt{x_i^2 + y_j^2} + h\right)$ in the two dimensions and $1/\left(\sqrt{x_i^2 + y_j^2 + z_k^2} + h\right)$ in the three dimensions [4]. From these arguments, we estimate the size of the difference of the two functions in L^∞ as

$$\left\| u_P^h - u_F^h + \left\langle 1^h, u_F^h \right\rangle_h 1^h \right\|_\infty = \left\langle b^h, 1^h \right\rangle_h \left\| G^h \right\|_\infty = \begin{cases} O\left(h^2 \left|\log h\right|\right) & \text{in } [0,1]^2, \\ O\left(h\right) & \text{in } [0,1]^3. \end{cases} \tag{11}$$

Taking the discrete gradient by the standard centered finite differences and applying the mean value theorem, we have

$$\nabla^x \left(\log\left(\sqrt{x_i^2 + y_j^2} + h\right)\right) = \frac{\tilde{x}_i}{\sqrt{\tilde{x}_i^2 + y_j^2}} \frac{1}{\sqrt{\tilde{x}_i^2 + y_j^2} + h} \quad \text{and}$$

$$\nabla^x \left(\frac{1}{\sqrt{x_i^2 + y_j^2 + z_k^2} + h}\right) = -\frac{\tilde{x}_i}{\sqrt{\tilde{x}_i^2 + y_j^2 + z_k^2}} \frac{1}{\left(\sqrt{\tilde{x}_i^2 + y_j^2 + z_k^2} + h\right)^2},$$

for some $\tilde{x}_i \in (x_i - h/2, x_i + h/2)$, and similarly taken are the cases of the other spatial derivatives. Using the fact that the pointwise error of the discrete and continuous fundamental functions is $O(1)$ for $d = 2$ ([10], [14]) and $O(h^{-1})$ for $d = 3$ ([4]), the difference of two gradients is hence estimated as

$$\left\| \nabla^h u_P^h - \nabla^h u_F^h \right\|_\infty = \left\langle b^h, 1^h \right\rangle_h \left\| \nabla^h G^h \right\|_\infty = \begin{cases} O\left(h\right) & \text{in } [0,1]^2, \\ O\left(1\right) & \text{in } [0,1]^3. \end{cases} \tag{12}$$

The standard finite difference method in two and three dimensional rectangular domains results in the following second order convergence of its numerical solution and gradient in L^∞,

$$\left\| u_P^h - u \right\|_\infty = O\left(h^2\right) \left(\int_\Omega u\, dx = 0\right) \quad \text{and} \quad \left\| \nabla^h u_P^h - \nabla u \right\|_\infty = O\left(h^2\right).$$

The estimations (11) and (12) lead to the following degraded convergence orders with the fixing method,

$$\left\|u_F^h - u + \left\langle 1^h, u_F^h \right\rangle_h 1^h\right\|_\infty = \begin{cases} O\left(h^2 \left|\log h\right|\right) & \text{in } [0,1]^2, \\ O\left(h\right) & \text{in } [0,1]^3 \end{cases}$$

and

$$\left\|\nabla^h u_F^h - \nabla u\right\|_\infty = \begin{cases} O\left(h\right) & \text{in } [0,1]^2, \\ O\left(1\right) & \text{in } [0,1]^3. \end{cases}$$

In Section 4 , the two estimations will be validated by the degraded convergence orders with the fixing method not only in the two-dimensional rectangular domains but also in three-dimensional and irregular domains.

3 Improvement of the fixing method

In the previous section, we showed that the fixing method gives rise to involve the function that has a singularity near the position of the Dirichlet boundary condition. The projection method is thus desired over the fixing method, but it involves some difficulties in its implementations. The conjugate gradient iteration step needs to include two additional projections per each iteration as follows, because its Krylov space should be confined in $\left\{1^h\right\}^\perp$

$$\begin{array}{lcl} \text{for} \quad n = 1, 2, \ldots, & & \\ \quad x^{n+1} & = & x^n + \frac{\langle r^n, r^n\rangle_h}{\langle p^n, A^h p^n\rangle_h} p^n; \\ \quad r^{n+1} & = & r^n - \frac{\langle r^n, r^n\rangle_h}{\langle p^n, A^h p^n\rangle_h} A^h p^n; \\ \quad r^{n+1} & = & r^{n+1} - \frac{\langle r^{n+1}, 1^h\rangle_h}{\langle 1^h, 1^h\rangle_h} 1^h; \ //\text{projection on } \left\{1^h\right\}^\perp \\ \quad p^{n+1} & = & r^{n+1} + \frac{\langle r^{n+1}, r^{n+1}\rangle_h}{\langle r^n, r^n\rangle_h} p^n; \\ \quad p^{n+1} & = & p^{n+1} - \frac{\langle 1^h, p^{n+1}\rangle_h}{\langle 1^h, 1^h\rangle_h} 1^h \ //\text{projection on } \left\{1^h\right\}^\perp \end{array}$$

Overcoming the extra procedures caused in the projection method, we suggest an improvement of the fixing method as

$$\left\{ \begin{array}{rcll} A^h u_I^h & = & P^h b^h & \text{in } \Omega^h \setminus \{Q\}, \\ u_I^h & = & 0 & \text{at } \{Q\}. \end{array} \right. \tag{13}$$

Note that its only difference from the fixing method is to take the right-hand side as $P^h b^h$, rather than b^h, which causes the system to be consistent.

Theorem 3.1 *The improved fixing method has the same solution as the projection method up to the addition of a constant function.*

Proof Let u_I^h be the solution to Equation (13). From the fact that $\ker(A^h) = span\{1^h\}$, it is enough to show that $A^h u_I^h = P^h b^h$ at Q. Since P^h is the projection onto the zero-mean space,

$$\sum_{X \in \Omega^h \setminus \{Q\}} \left(P^h b^h\right)(X) = 0 - \left(P^h b^h\right)(Q).$$

Also, since $R(A^h) = \left\{1^h\right\}^\perp$, $A^h u_I^h$ has mean zero so that we have

$$\sum_{X \in \Omega^h \setminus \{Q\}} \left(A^h u_I^h\right)(X) = 0 - \left(A^h u_I^h\right)(Q).$$

On the other hand, the definition of u_I^h given in Equation (13) shows that $\left(A^h u_I^h\right)(X) = \left(P^h b^h\right)(X)$ for all $X \in \Omega^h \setminus \{Q\}$. Equating the two summations, we conclude that $A^h u_I^h = P^h b^h$ at Q. ∎

By the theorem above, compared to the projection method that deals with semi-definite matrix, our suggested improved fixing method deals with a postive-definite matrix without changing the solution. We note that there are pros and cons between the two methods. While the projection method results in a singular matrix, the improved method results in a nonsingular matrix, that is a principal submatrix of the singular matrix A^h. However the improved method still suffers from the drawback of a worse condition number than the projection method. Let us review the following standard argument about the condition number. We denote by A^h_Q the submatrix obtained from deleting the row and column of A^h related to the fixing point Q. Let $0 = \lambda_1 < \lambda_2 \leq \cdots \leq \lambda_n$ be the eigenvalues of A^h, and let $0 < \mu_1 < \mu_2 \leq \cdots \leq \mu_{n-1}$ be the eigenvalues of A^h_Q,. According to the Cauchy interlace theorem [17, 11], we have $0 = \lambda_1 < \mu_1 \leq \lambda_2$ and $\lambda_{n-1} \leq \mu_{n-1} \leq \lambda_n$.

Theorem 3.2 *The condition numbers of matrices A^h and A^h_Q are related as*

$$\left|\frac{\mu_{n-1}}{\mu_1}\right| = \left|\frac{\lambda_n}{\lambda_2}\right| \cdot \begin{cases} O\left(|\log h| + 1\right) & \text{in } \mathbb{R}^2 \\ O\left(\frac{1}{h}\right) & \text{in } \mathbb{R}^3. \end{cases}$$

Proof See Theorem 5.2 in [2]. ∎

4 Numerical experiments

In the previous section, we analyzed the difference between the projection method and the one-point fixing method in rectangular domains. In this section, we validate the analysis through numerical experiments in Example 1 and Example 3. Example 2 and Example 4 test if the argument of the analysis is still valid in irregular domains.

The projection method and the improved fixing method generate the same solution within the machine epsilon, according to Theorem 3.1. Therefore, we report only one of them in accuracy calculation and graph visualization. Each linear system is solved by the conjugate gradient algorithm with stopping criterion $\|r^n\|_{L^2} < \|r^0\|_{L^2} \cdot 10^{-15}$.

Example 1 : Rectangular domain in $\mathbb{R}^2$

The Neumann problem with exact solution $u(x,y) = e^x \sin(y))$ and $\Omega = [0,1]^2$ is solved by the standard 5-point finite difference method. The fixing one-point method imposes the Dirichlet boundary condition at $(0,0)$. Table 1 reports the second order convergence of the projection method as follows:

$$\begin{aligned} \left\|u^h_P - u\right\|_\infty &= O\left(h^2\right), \\ \left\|\nabla^h u^h_P - \nabla u\right\|_\infty &= O\left(h^2\right), \\ \left\|\nabla^h u^h_P - \nabla u\right\|_{L^2} &= O\left(h^2\right). \end{aligned}$$

According to the analysis and argument in Section 2 and applying the triangle inequality, we expect the degraded accuracy of the fixing method as

$$\begin{aligned} \left\|u^h_F - \bar{u}_F - u\right\|_\infty &= O\left(h^2\right) + O\left(h^2 |\log h|\right) = O\left(h^2 |\log h|\right), \\ \left\|\nabla^h u^h_F - \nabla u\right\|_\infty &= O\left(h^2\right) + O\left(h\right) = O\left(h\right), \\ \left\|\nabla^h u^h_F - \nabla u\right\|_{L^2} &= O\left(h^2\right) + O\left(h^2\sqrt{|\log h|}\right) = O\left(h^2\sqrt{|\log h|}\right). \end{aligned}$$

Table 2 validates the expectation. Note that either $O\left(h^2 |\log h|\right)$ or $O\left(h^2\sqrt{|\log h|}\right)$ is so similar to $O\left(h^2\right)$ that the order of two is slightly diminished in the table. Table 3 confirms Theorem 3.2, since larger condition number yields slower performance of the CG algorithm. Figure 1 illustrates Equations (9, 11,12) stating that that the difference $u^h_P - \left(u^h_F - \bar{u}^h_F\right)$ has a singularity at the position of the Dirichlet boundary condition.

	$\|u-u_P^h\|_\infty$	order	$\|\nabla u-\nabla^h u_P^h\|_\infty$	order	$\|\nabla u-\nabla^h u_P^h\|_{L^2}$	order
1/10	4.89E-04	-	4.21E-04	-	2.60E-04	-
1/20	1.29E-04	1.92	1.11E-04	1.93	6.57E-05	1.99
1/40	3.32E-05	1.96	2.83E-05	1.97	1.65E-05	2.00
1/80	8.42E-06	1.98	7.16E-06	1.98	4.12E-06	2.00
1/160	2.12E-06	1.99	1.80E-06	1.99	1.03E-06	2.00

Table 1: Convergence orders of the projection method in Example 1

	$\|u-u_F^h+\bar{u}_F\|_\infty$	order	$\|\nabla u-\nabla^h u_F^h\|_\infty$	order	$\|\nabla u-\nabla^h u_F^h\|_{L^2}$	order
1/10	1.53E-03	-	3.44E-03	-	8.45E-04	-
1/20	4.62E-04	1.72	1.67E-03	1.04	2.38E-04	1.83
1/40	1.34E-04	1.78	8.26E-04	1.01	6.55E-05	1.86
1/80	3.82E-05	1.81	4.12E-04	1.00	1.77E-05	1.88
1/160	1.07E-05	1.83	2.06E-04	1.00	4.75E-06	1.90

Table 2: Convergence orders of the fixing method in Example 1

h	1/10	1/20	1/40	1/80	1/160
Projection method	47	103	226	455	911
Fixing one point method	70	151	309	717	1484
Improved fixing method	70	151	327	660	1484

Table 3: Iteration number of CG in Example 1

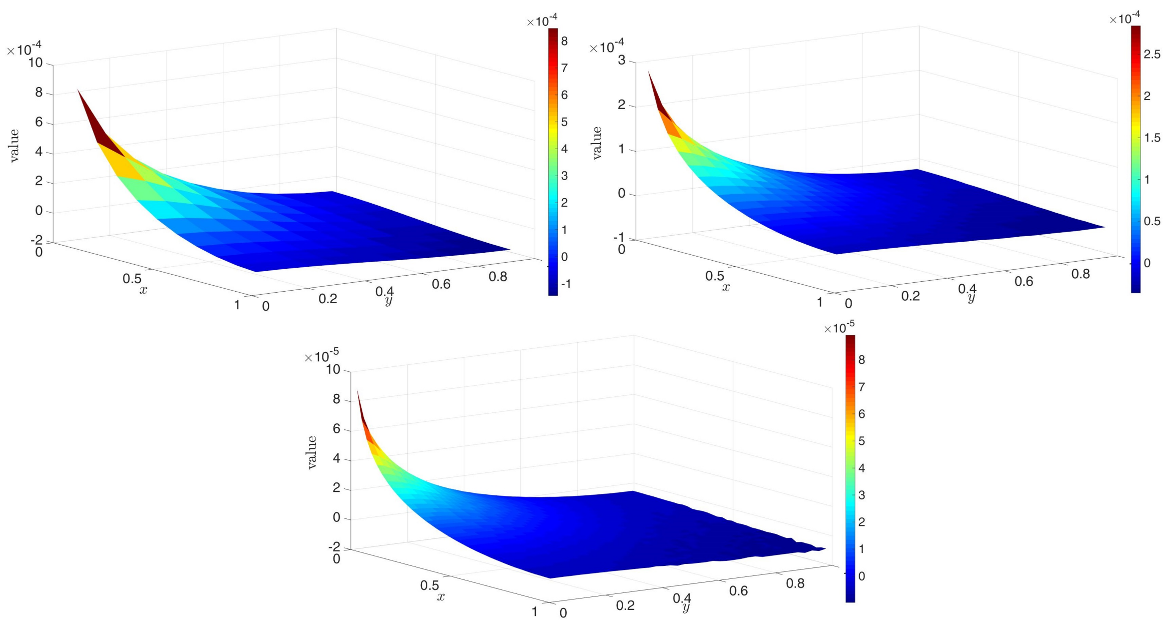

Figure 1: Graph of $u_P^h-\left(u_F^h-\bar{u}_F\right)$ for $h=1/10,1/20,1/40$ in Example 1

Example 2 : Irregular domain in $\mathbb{R}^2$

The Neumann problem with exact solution $u(x,y) = \sin(x)\sin(y) - 4\sin^4(1/2)$ and $\Omega = \left\{(x,y) \,|x^2+y^2<1\right\}$ is solved by the standard 5-point finite volume method. The fixing one-point method and the improved fixing method imposes Dirichlet boundary condition at $(0,0)$. Table 4 reports the convergence orders of the projection method as

$$\begin{aligned}\left\|u_P^h - u\right\|_\infty &= O\left(h^2\right)\\ \left\|\nabla^h u_P^h - \nabla u\right\|_\infty &= O(h)\\ \left\|\nabla^h u_P^h - \nabla u\right\|_{L^2} &= O\left(h^{1.5}\right).\end{aligned}$$

Though the last column in Table 4 reveals no clear sign of convergence order, there exists a convergence analysis $\left\|\nabla^h u_P^h - \nabla u\right\|_{L^2} = O\left(h^{1.5}\right)$ [21]. Even though the analysis and argument in Section 2 was carried out for regular domains, the main argument is deeply involved in the Green function G^h which still exists in irregular domains. Therefore we may apply the analysis and argument to irregular domains and expect the following degraded accuracies of the fixing method. Our expectation is supported and validated by the numerical results given in Table 5.

$$\begin{aligned}\left\|u_F^h + \bar{u}_F - u\right\|_\infty &= O\left(h^2\right) + O\left(h^2\left|\log h\right|\right) = O\left(h^2\left|\log h\right|\right)\\ \left\|\nabla^h u_F^h - \nabla u\right\|_\infty &= O(h) + O(h) = O(h)\\ \left\|\nabla^h u_F^h - \nabla u\right\|_{L^2} &= O\left(h^{1.5}\right) + O\left(h^2\sqrt{\left|\log h\right|}\right) = O\left(h^{1.5}\right).\end{aligned}$$

Table 6 shows that the two fixing methods, which share the same matrix, have worse condition number than the projection method. This suggests that Theorem 3.2 is still valid in irregular domains. Figure 2 illustrates Equations (9, 11,12) stating that that the difference $u_P^h - \left(u_F^h - \bar{u}_F^h\right)$ has a singularity at the position of the Dirichlet boundary condition.

	$\|u-u_P^h\|_\infty$	order	$\|\nabla u - \nabla^h u_P^h\|_\infty$	order	$\|\nabla u - \nabla^h u_P^h\|_{L^2}$	order
$\sqrt{2}/20$	1.52E-03		2.43E-02		5.98E-03	
$\sqrt{2}/40$	3.85E-04	1.98	5.15E-03	2.24	1.20E-03	2.32
$\sqrt{2}/80$	9.31E-05	2.05	6.03E-03	-0.23	6.20E-04	0.95
$\sqrt{2}/160$	2.41E-05	1.95	3.27E-03	0.88	1.64E-04	1.91
$\sqrt{2}/320$	6.05E-06	1.99	1.58E-03	1.05	5.07E-05	1.70

Table 4: Convergence orders of the projection method in Example 2

	$\|u-u_F^h+\bar{u}_F\|_\infty$	order	$\|\nabla u - \nabla^h u_F^h\|_\infty$	order	$\|\nabla u - \nabla^h u_F^h\|_{L^2}$	order
$\sqrt{2}/20$	1.63E-03		2.44E-02		6.32E-03	
$\sqrt{2}/40$	4.17E-04	1.96	5.16E-03	2.24	1.30E-03	2.28
$\sqrt{2}/80$	1.16E-04	1.84	6.03E-03	-0.23	6.33E-04	1.04
$\sqrt{2}/160$	3.33E-05	1.80	3.27E-03	0.88	1.68E-04	1.91
$\sqrt{2}/320$	9.20E-06	1.85	1.58E-03	1.05	5.15E-05	1.71

Table 5: Convergence orders of the fixing one-point method in Example 2

Example 3 : Rectangular domain in $\mathbb{R}^3$

The Neumann problem with exact solution $u(x,y,z) = e^{x^2}\left(y^2+\cos(z)\right)$ and $\Omega = [0,1]^3$ is solved by the standard 7-point finite difference method. The fixing one-point method and the improved fixing

h	$\sqrt{2}/20$	$\sqrt{2}/40$	$\sqrt{2}/80$	$\sqrt{2}/160$	$\sqrt{2}/320$
Projection method	92	182	344	648	1382
Fixing one point method	147	284	559	1096	2117
Improved fixing method	147	298	536	1096	2117

Table 6: Iteration number of CG in Example 2

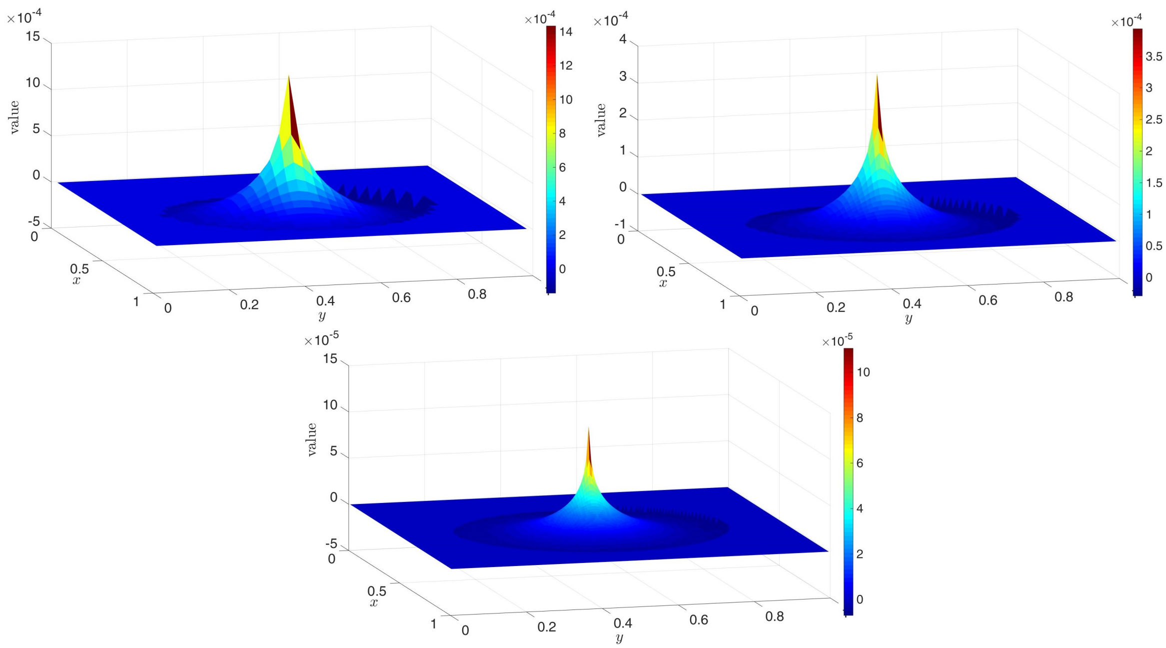

Figure 2: Graph of $u_P^h - \left(u_F^h - \bar{u}_F\right)$ for $h = \sqrt{2}/20, \sqrt{2}/40, \sqrt{2}/80$ in Example 2

method imposes Dirichlet boundary condition at $(0,0,0)$. Table 7 reports the convergence orders of the projection method as

$$\begin{aligned}
\left\|u_P^h - u\right\|_\infty &= O\left(h^2\right) \\
\left\|\nabla^h u_P^h - \nabla u\right\|_\infty &= O\left(h^2\right) \\
\left\|\nabla^h u_P^h - \nabla u\right\|_{L^2} &= O\left(h^2\right).
\end{aligned}$$

According to the analysis and argument in Section 2, we expect the degraded accuracy of the fixing method as

$$\begin{aligned}
\left\|u_F^h - \bar{u}_F - u\right\|_\infty &= O\left(h^2\right) + (h) = O(h) \\
\left\|\nabla^h u_F^h - \nabla u\right\|_\infty &= O\left(h^2\right) + O(1) = O(1) \\
\left\|\nabla^h u_F^h - \nabla u\right\|_{L^2} &= O\left(h^2\right) + O\left(h^{1.5}\right) = O\left(h^{1.5}\right),
\end{aligned}$$

which is clearly verified by Table 8. Table 9 shows that the two fixing methods, which share the same matrix, have worse condition number than the projection method, which confirms Theorem 3.2.

	$\lVert u - u_P^h\rVert_\infty$	order	$\lVert \nabla u - \nabla^h u_P^h\rVert_\infty$	order	$\lVert \nabla u - \nabla^h u_P^h\rVert_{L^2}$	order
$1/10$	3.01E-03	-	1.56E-02	-	7.59E-03	-
$1/20$	7.69E-04	1.97	4.03E-03	1.96	1.91E-03	1.99
$1/40$	1.93E-04	2.00	1.02E-03	1.98	4.78E-04	2.00
$1/80$	4.83E-05	2.00	2.57E-04	1.99	1.19E-04	2.00
$1/160$	1.21E-05	2.00	6.45E-05	2.00	2.99E-05	2.00

Table 7: Convergence orders of the projection method in Example 3

	$\lVert u - u_F^h + \bar{u}_F\rVert_\infty$	order	$\lVert \nabla u - \nabla^h u_F^h\rVert_\infty$	order	$\lVert \nabla u - \nabla^h u_F^h\rVert_{L^2}$	order
$1/10$	1.80E-01	-	9.01E-01	-	6.93E-02	-
$1/20$	9.38E-02	0.94	9.03E-01	-0.00	2.52E-02	1.46
$1/40$	4.79E-02	0.97	9.04E-01	-0.00	9.00E-03	1.48
$1/80$	2.42E-02	0.99	9.04E-01	-0.00	3.20E-03	1.49
$1/160$	1.21E-02	0.99	9.04E-01	-0.00	1.13E-03	1.50

Table 8: Convergence orders of the fixing one-point method in Example 3

h	$1/10$	$1/20$	$1/40$	$1/80$	$1/160$
Projection method	56	124	256	555	1172
Fixing one point method	110	236	481	1176	2014
Improved fixing method	110	236	481	961	2012

Table 9: Iteration number of CG in Example 3

Example 4 : Irregular domain in $\mathbb{R}^3$

The Neumann problem with exact solution $u(x,y,z) = \sin(x+y)\, e^{-xyz}$ and $\Omega = \left\{(x,y,z)\,|x^2+y^2+z^2<1\right\}$ is solved by the standard finite volume method. The fixing one-point method and the improved fixing method imposes Dirichlet boundary condition at $(0,0,0)$. Table 10 reports the convergence orders of the projection method as

$$\begin{aligned} \left\|u_P^h - u\right\|_{L^\infty} &= O\left(h^2\right) \\ \left\|\nabla^h u_P^h - \nabla u\right\|_{L^\infty} &= O\left(h\right) \\ \left\|\nabla^h u_P^h - \nabla u\right\|_{L^2} &= O\left(h^{1.5}\right). \end{aligned}$$

Though the last column in Table 10 seems to indicate higher convergence order than $O\left(h^{1.5}\right)$, there exists a convergence analysis $\left\|\nabla^h u_P^h - \nabla u\right\|_{L^2} = O\left(h^{1.5}\right)$ [21]. As mentioned in Example 2, we may apply the analysis and argument to irregular domains and expect the following degraded accuracies of the fixing method. Our expectation is supported and validated by the numerical results given in Table 11.

$$\begin{aligned} \left\|u_F^h - \bar{u}_F - u\right\|_\infty &= O\left(h^2\right) + O\left(h\right) = O\left(h\right) \\ \left\|\nabla^h u_F^h - \nabla u\right\|_\infty &= O\left(h\right) + O\left(1\right) = O\left(1\right) \\ \left\|\nabla^h u_F^h - \nabla u\right\|_{L^2} &= O\left(h^{1.5}\right) + O\left(h^{1.5}\right) = O\left(h^{1.5}\right). \end{aligned}$$

Table 6 shows that the two fixing methods, which share the same matrix, have similar condition number than the projection method.

	$\\|u - u_P^h\\|_\infty$	order	$\\|\nabla u - \nabla^h u_P^h\\|_\infty$	order	$\\|\nabla u - \nabla^h u_P^h\\|_{L^2}$	order
$\sqrt{2}/5$	1.51E-01		2.01E-01		2.11E-01	
$\sqrt{2}/10$	3.19E-02	2.24	6.58E-02	1.61	5.22E-02	2.02
$\sqrt{2}/20$	5.70E-03	2.48	2.90E-02	1.18	1.27E-02	2.04
$\sqrt{2}/40$	1.37E-03	2.06	1.35E-02	1.10	3.29E-03	1.95
$\sqrt{2}/80$	3.36E-04	2.02	7.08E-03	0.93	8.86E-04	1.89

Table 10: Convergence order of the projection method in Example 4

	$\\|u - u_F^h + \bar{u}_F\\|_\infty$	order	$\\|\nabla u - \nabla^h u_F^h\\|_\infty$	order	$\\|\nabla u - \nabla^h u_F^h\\|_{L^2}$	order
$\sqrt{2}/5$	8.40E-02		2.95E-01		2.27E-01	
$\sqrt{2}/10$	4.98E-02	0.75	2.63E-01	0.17	6.55E-02	1.79
$\sqrt{2}/20$	2.64E-02	0.92	2.54E-01	0.05	1.92E-02	1.77
$\sqrt{2}/40$	1.34E-02	0.97	2.53E-01	0.01	6.07E-03	1.66
$\sqrt{2}/80$	6.76E-03	0.99	2.53E-01	0.00	2.01E-03	1.60

Table 11: Convergence orders of the fixing one-point method in Example 4

h	$\sqrt{2}/5$	$\sqrt{2}/10$	$\sqrt{2}/20$	$\sqrt{2}/40$	$\sqrt{2}/80$
Projection method	247	678	923	2572	2072
Fixing one point method	223	647	990	2561	2371
Improved fixing method	224	649	990	2734	2375

Table 12: Iteration number of CG in Example 4

5 Conclusion

We compared two approaches handling the singularity of the linear system associated with the Poisson equation with the Neumann boundary condition. One is to fix the Dirichlet boundary condition at one point, and the other seeks a unique solution in the orthogonal complement of the kernel. We showed that the two solutions differ by a function that has a singularity pole as large as that of the fundamental solution of the Laplace operator. The pole turns out to severely corrupt the accuracy of the numerical solution and its gradient of the fixing method.

We presented the numerical analysis on the standard finite difference method in the unit volumes in $\mathbb{R}^2$ and $\mathbb{R}^3$. Other numerical methods seem to behave similarly, one of which was presented with numerical evidences. The missing analysis of the other numerical methods is currently beyond our capacity, and we put it off to future work. The argument in this work may be obviously extended to other spatial dimensions. However, we restricted our attentions to two and three dimensions in which Poisson equations are usually set. Due to the limit of time available to us, we leave the discussion of other dimensions as a future work.

The projection method on the orthogonal space deals with semi-definite matrix, due to which the iterative method needs to include two additional inner-products for each step. We suggested a simple improved fixing method that has the same numerical method as the projection method and involves a positive-definite matrix. However, the positive-definite matrix has a worse condition number than the semi-definite matrix by a ratio of $|\ln h|$. It is uncertain to definitely prefer one between the projection method and the improved fixing method, and we leave the choice to the users.

Acknowledgement

We greatly thank and acknowledge the reviewers for their comments which helped us to improve and clarify the manuscript.

References

[1] H. Ammari, H. Kang, and S. Kim, *Sharp estimates for the Neumann functions and applications to quantitative photo-acoustic imaging in inhomogeneous media*, J. Diff. Eq. 253 (2012), 41–72.

[2] P. Bochev and R. B. Lehoucq, *On the finite element solution of the pure Neumann problem,* SIAM Rev. 47 (2005), 50–66.

[3] J. H. Bramble, J. E. Pasciak, and A. H. Schatz, *The construction of preconditioners for elliptic problems by substructuring I,* Math. Comp. 47 (1986), 103–134.

[4] J. H. Bramble and V. Thomee, *Pointwise bounds for discrete Green's functions,* SIAM J. Numer. Anal. 6 (1969), 583–590.

[5] S. Brenner and R. Scott, *The mathematical theory of finite element methods,* Springer-Verlag, New York, 1994.

[6] R. Bridson, *Fluid simulation for computer graphics,* CRC Press, 2008.

[7] C. R. Deeter and J. M. Gray, *The discrete Green's function and the discrete kernel function,* Discrete Math. (1974), 29–42.

[8] L. C. Evans, *Partial differential equations,* Amer. Math. Soc., 1998.

[9] M. S. Gockenbach, *Understanding and implementing the finite element method,* SIAM, Philadelphia, 2006.

[10] K. Gürlebeck and A. Hommel, *On the finite difference potentials and their applications in a discrete function theory,* Math. Meth. Appl. Sci. 25(2002), 1563–1576.

[11] S.-G. Hwang, *Cauchy's interlace theorem for eigenvalues of Hermitian matrices,* Amer. Math. Mon. 111 (2004), 157–159.

[12] C. E. Kenig, *Harmonic analysis techniques for second order elliptic boundary value problems*, Amer. Math. Soc., Providence, RI, 1994.

[13] T. Kolokolnikov, M. J. Ward, and J. Wei, *Spot Self-Replication and Dynamics for the Schnakenburg Model in a Two-Dimensional Domain,* J. Nonlinear Sci. 19 (2009), 1–56.

[14] P. Laasonen, *On the solution of Poisson's difference equation,* J. Assoc. Comput. Mach. 5(1958), 370–382.

[15] G. F. Lawler and V. Limic, *Random walk: a modern introduction,* Cambridge Studies in Advanced Mathematics 123, Cambridge University Press, Cambridge, 2010.

[16] Y. T. Ng, C. Min, F. Gibou, *An efficient fluid–solid coupling algorithm for single-phase flows*, J. Comput. Phys., 228, (2009), 8807–8829.

[17] B. N. Parlett, *The symmetric eigenvalue problem,* Prentice-Hall, Inc., 1998.

[18] J. W. Purvis and J. E. Burkhalter, *Prediction of critical mach number for store configurations,* AIAA J., 17, (1979), 1170–1177.

[19] Y. Saad, *Iterative Methods for Sparse Linear Systems,* SIAM, Philadelphia, 2003.

[20] J. W. Thomas, *Numerical partial differential equations: conservation laws and elliptic equations,* Springer-Verlag New York, 1999.

[21] G. Yoon, J.-H. Park, and C. Min, *Convergence analysis on the Gibou-Min method for the Hodge projection,* submitted to Comm. Math. Sci.